ISLAMIC UNIVERSITY OF TECHNOLOGY

DEPARTMENT OF ELECTRICAL AND ELECTRONIC ENGINEERING
GAZIPUR, BANGLADESH

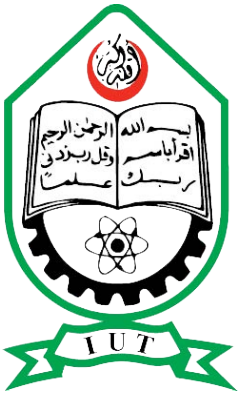

Design and Analysis of Air Gap Based Semi-Elliptical Coupler

BY

Md. Saiful Islam Sumon
ID: 142401

Mahir Tazwar
ID: 142405

Sakib Mahtab Khandaker
ID: 142408

A THESIS SUBMITTED TO THE ACADEMIC FACULTY IN PARTIAL FULFILLMENT OF THE REQUIREMENTS FOR THE DEGREE OF

BACHELOR OF SCIENCE IN ELECTRICAL AND ELECTRONIC ENGINEERING

November 12, 2018

Design and Analysis of Semi-Elliptical Coupler and Plasmonic Gates

Approved by:

Dr. Rakibul Hasan Sagor

Supervisor and Assistant Professor,
Department of Electrical and Electronic Engineering,
Islamic University of Technology (IUT),
Boardbazar, Gazipur - 1704.

Date: .....

Prof. Dr. Md. Ashraful Hoque

Head of the Department,
Department of Electrical and Electronic Engineering,
Islamic University of Technology (IUT),
Boardbazar, Gazipur - 1704.

Date: .....

Contents

List of Figures

List of Tables

ACKNOWLEDGEMENTS

First and foremost, we offer our gratitude to the Almighty Allah (SWT) for bestowing us the competence to do this thesis in good health.

We are grateful to our research supervisor, Dr. Rakibul Hasan Sagor, for the support and guidance throughout our research. He created a pleasant research environment thanks to which we were able to explore many ideas without restriction. We have gained a wealth of knowledge and experience in plasmonics and research methodology through his supervision. For all of his efforts to make us better students, better researchers and most importantly better humans.

We would also like to thank all the faculty members of the department of EEE, IUT for their inspiration and help. Lastly we are thankful to our family, friends and well-wishers for their support and inspiration. Without them it would be very challenging for us to complete this goal.

ABSTRACT

Efficient coupling of light between the dielectric waveguide and plasmonic waveguide has been investigated theoretically in three dimensions. An air gap based nanoplasmonic semi-elliptical structure of Silicon (Si) is used as a coupler which connects these waveguides. Finite Integration Technique (FIT) has been deployed for this investigation. Theoretical coupling efficiency of $\sim$ 85% at optical communication wavelength (1.55 μm) has been achieved through numerical simulations. The dependency of coupling efficiency has been investigated by varying the curvature of the semi-elliptical coupler, the air gap width between the two waveguides and the plasmonic width of the Ag-Air-Ag waveguide, and an optimal dimension of the proposed structure has been obtained. Different performance parameters like coupling efficiency, reflection coefficient, Voltage Standing Wave Ratio (VSWR), and return loss have been analyzed with the obtained optimal dimensions. Broad range of operating frequency, tolerance to angular and air gap misalignment and excellent agreement to a demonstrated experimental coupler has made the proposed coupler distinctive.

Chapter 1

INTRODUCTION

Plasmonics, capable of unifying electronics and photonics [1], is one of the promising sub-disciplines of Nano-photonics, which has attracted much attention in recent years due to its incredible ability to suppress diffraction limit. This limit is a critical challenge to the manipulation of light in subwavelength scales (i.e. scales much smaller than the wavelength of light) [2]. Consequent achievement of which is the localized electromagnetic energy (at communication wavelength) into nanoscale regions as little as just a few nanometers [3]. Plasmonics with its unprecedented ability of light confinement and substantial light-matter interactions has already opened up many opportunities like subwavelength imaging and superlenses [4], chemical and biological sensing [5], plasmonic solar cells [6], plasmonic metamaterials [7], plasmonic nanostructures with DNA [8], self-assembly [9] and so on. These interdisciplinary applications prospects how far plasmonics can go.

1.1 Overview of Surface Plasmon Polariton

Surface plasmon polaritons are electromagnetic excitations propagating at the interface between a dielectric and a conductor, evanescently confined in the perpendicular direction. These electromagnetic surface waves arise via the coupling of the

electromagnetic fields to oscillations of the conductors electron plasma.

The eigen modes of an interface between a dielectric and a metal are surface plasmon polaritons (SPPs). We refer to them as eigen modes in the sense that they are solutions of Maxwell's equations that can be formulated in the absence of an incident field. On a flat interface between dielectric and metal half-spaces with dielectric constants d and m, respectively, SPPs are transverse magnetic (TM) plane waves propagating along the interface. Assuming the interface is normal to z and the SPPs propagate along the x direction, the SPP wave vector is related to the optical frequency through the dispersion relation,

$$k_x = k_o \sqrt{\frac{\epsilon_d \epsilon_m}{\epsilon_d + \epsilon_m}} \tag{1.1}$$

Where k_o is the free space wave vector. We take to be real and allow to be complex, since our main interest is in stationary monochromatic SPP fields in a finite area.

1.2 Literature Review

Plasmonic waveguides have been anticipated to be an eligible candidate for the upcoming highly-integrated photonic circuits. Several distinct plasmonic waveguides have been proposed and analyzed so far, such as metal nanoparticle plasmon waveguides [10], integrated metal slot waveguide [11], hybrid plasmonic waveguides [2, 12], stripe waveguides [13] and so on. Particularly, Metal-Dielectric-Metal (MDM) plasmonic waveguide has the incredible ability to guide optical signals in subwavelength scale through Surface Plasmon Polaritons (SPPs). Research work on MDM configuration of SPP waveguides has made major advances in superlens [14], hyperlens [15], combiners [16], splitters [17], Bragg reflectors [18] and many more.

Above all, there is a trade-off between the mode confinement and propagation length of these MDM plasmonic waveguides. This limitation of propagation length is due to the propagation loss of SPP in one of the major constituent material, metal. To overcome this problem it is imperative to use both dielectric waveguide and MDM waveguide in the same platform. Propagation loss will be compensated by the dielectric waveguide and for dealing with subwavelength scale optoelectronic devices, MDM waveguides will be utilized. Thus, it is indispensable to place a coupler between the two waveguides following the essence of efficient coupling between them. Several techniques for efficient coupling have been proposed like nano-plasmonic coupler with multi-section tapers [19], nanoplasmonic air-slot coupler [20], $\lambda/4$ coupler [21], adiabatic and non-adiabatic tapered plasmonic coupler [22] etc.

Main focus has been given on designing the semi-elliptical coupler. An air gap based nanoplasmonic semi-elliptical structure of Silicon (Si) is used as a coupler which connects these waveguides. Finite Integration Technique (FIT) has been deployed for this investigation. Theoretical coupling efficiency of $\sim$ 85% at optical communication wavelength (1.55 μm) has been achieved through numerical simulations. The dependency of coupling efficiency has been investigated by varying the curvature of the semi-elliptical coupler, the air gap width between the two waveguides and the plasmonic width of the Ag-Air-Ag waveguide, and an optimal dimension of the proposed structure has been obtained. Different performance parameters like coupling efficiency, reflection coefficient, Voltage Standing Wave Ratio (VSWR), and return loss have been analyzed with the obtained optimal dimensions. Broad range of operating frequency, tolerance to angular and air gap misalignment and excellent agreement to a demonstrated experimental coupler has made the proposed coupler distinctive.

1.3 Thesis Objective

The main objective of the thesis is to accomplish novel and optimum designs of plasmonic nanostructures with pragmatic applications. In short the objectives can be described as follows:

- Implementing FIT algorithm and dispersion parameters of materials in CST Microwave Studio (CST MWS).
- Designing the Semi-elliptical coupler with uniform air-gap
- Obtaining the optimum dimensions of the coupler
- Determining the performance parameters of the coupler such as coupling efficiency, reflection coefficient, Voltage Standing Wave Ratio (VSWR), and return loss.
- Obtaining the relative permitivity of heavily doped InP (Indium Phosphide) for different doping concentration.
- Exploring performance of different plasmonic gates

Chapter 2

SPP Propagation Theory

2.1 Introduction

Surface Plasmon Polaritons (SPP) are electromagnetic excitation that propagate in a wave like manner along a metal-dielectric medium (the dielectric could be a vacuum or air). It involves both charge motion in the metal (surface plasmon) and electromagnetic waves in the dielectric (polariton). Plasmons, which are longitudinal electron density oscillations, resemble light waves confined to the surface of a metal.

Electromagnetic wave propagation is obtained from the solution of Maxwells equation in each medium, and the associated boundary conditions. Maxwells equations of macroscopic electromagnetism are presented below.

From Gauss's Law for the electric field,

$$\nabla.D = \rho_{ext} \tag{2.1}$$

From Gauss's Law for the magnetic field,

$$\nabla.B = 0 \tag{2.2}$$

From Faraday's Law,

$$\nabla \times E = -\frac{\partial B}{\partial t} \tag{2.3}$$

From Ampere's Law,

$$\nabla \times H = \mathrm{J_{ext}} + \frac{\partial B}{\partial t} \tag{2.4}$$

Here,

E is the electric field vector in volt per meter

D is the electric flux density vector in coulombs per square meter

H is the magnetic field vector in amperes per meter

B is the magnetic flux density vector in webbers per square meter

ρ_{ext} is the charge density

$\mathrm{J_{ext}}$ is the current density

2.2 SPP at Single Interface

The simplest configuration for SPP propagation is at a single interface. This is between a dielectric of dielectric constant ϵ_2 and a metal of negative dielectric constant ϵ_1. For the metal, the bulk plasmon frequency will be ω and the amplitude decays perpendicular to the z-direction.

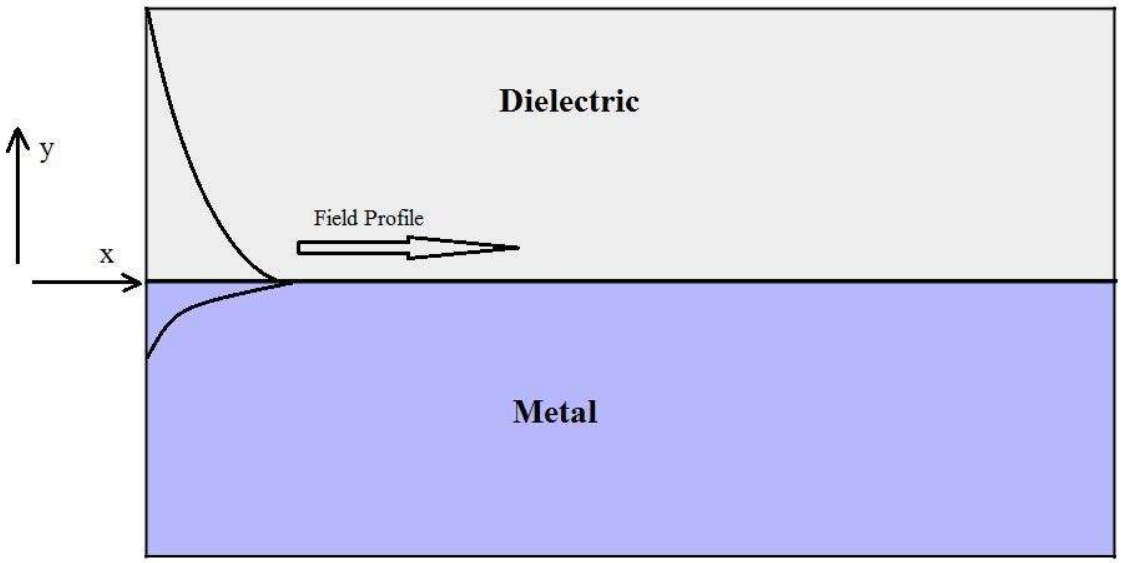

Figure 2.1: SPP propagation at the single interface

2.3 SPP at Double Interface

The two most prominent double interface configurations of SPP waveguides are the Metal-Dielectric-Metal (MDM) and Dielectric-Metal-Dielectric (DMD). In these cases, SPPs are formed on both interfaces. When the distance is shorted than decay distance, it forms coupled mode of SPP. This coupled mode of propagation can be also be sub-divided into even and odd modes, as shown in the figure 2.2.

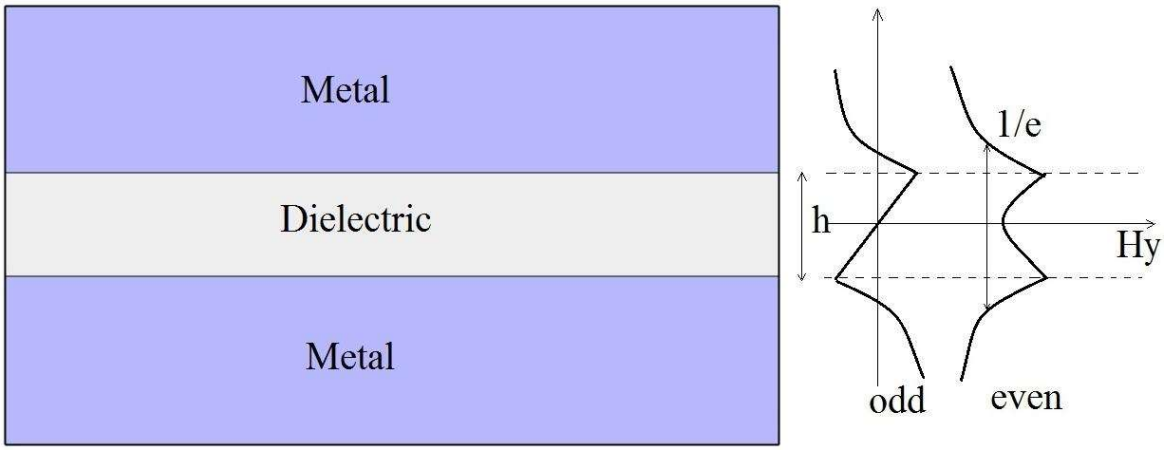

Figure 2.2: SPP propagation at double interface

Chapter 3

SEMI-ELLIPTICAL COUPLER

3.1 Introduction

Plasmonic waveguides have been anticipated to be an eligible candidate for the upcoming highly-integrated photonic circuits. Several distinct plasmonic waveguides have been proposed and analyzed so far, such as metal nanoparticle plasmon waveguides [10], integrated metal slot waveguide [11], hybrid plasmonic waveguides [2, 12], stripe waveguides [13] and so on. Particularly, Metal-Dielectric-Metal (MDM) plasmonic waveguide has the incredible ability to guide optical signals in subwavelength scale through Surface Plasmon Polaritons (SPPs). Research work on MDM configuration of SPP waveguides has made major advances in superlens [14], hyperlens [15], combiners [16], splitters [17], Bragg reflectors [18] and many more.

Above all, there is a trade-off between the mode confinement and propagation length of these MDM plasmonic waveguides. This limitation of propagation length is due to the propagation loss of SPP in one of the major constituent material, metal. To overcome this problem it is imperative to use both dielectric waveguide and MDM waveguide in the same platform. Propagation loss will be compensated by the dielectric waveguide and for dealing with subwavelength scale optoelectronic devices, MDM waveguides will be utilized. Thus, it is indispensable to place a coupler between the two waveguides following the essence of efficient coupling between them. Several techniques for efficient coupling have been proposed like nano-plasmonic coupler with multi-section tapers [19], nanoplasmonic air-slot cou-

pler [20], $\lambda/4$ coupler [21], adiabatic and non-adiabatic tapered plasmonic coupler [22] etc.

In this paper, a novel design of an air gap based three-dimensional nanoplasmonic semi-elliptical coupler has been proposed along with the analysis of several performance parameters such as coupling efficiency, reflectance, absorbance, reflection coefficient, return loss and VSWR. Employing finite integration technique (FIT), a coupling efficiency of $\sim$ 85% has been achieved in the telecommunication wavelength (1.55 μm). The proposed coupler has been designed following the simulation of the experimentally investigated air-slot coupler of Rami A. Wahsheh *et al.* [23]. We have found excellent agreement between our reproduced coupler and the experimental coupler of Rami A. Wahsheh *et al.* [23]. Afterwards modifications are done accordingly to get our proposed efficient air gap nanoplasmonic semi-elliptical coupler.

To the best of our knowledge, this is for the first time, an air gap nanoplasmonic semi-elliptical coupler is proposed with three-dimensional analysis. Broad range of operating frequency, higher efficiency, and three-dimensional analysis are the key advantages that our proposed coupler is going to provide. Tolerance to angular and air gap misalignment has made our coupler distinctive, giving much flexibility to the fabrication process.

3.2 Air Gap Based Semi-Elliptical Coupler Design

An air gap based semi-elliptical coupler in three-dimension has been considered for coupling the dielectric waveguide with a metal-dielectric-metal (MDM) plasmonic waveguide. The MDM plasmonic waveguide is formed after sandwiching air (insulator) in between two silver (metal) plates. The geometry designated with the labels of the proposed structure is shown in fig. 3.1.

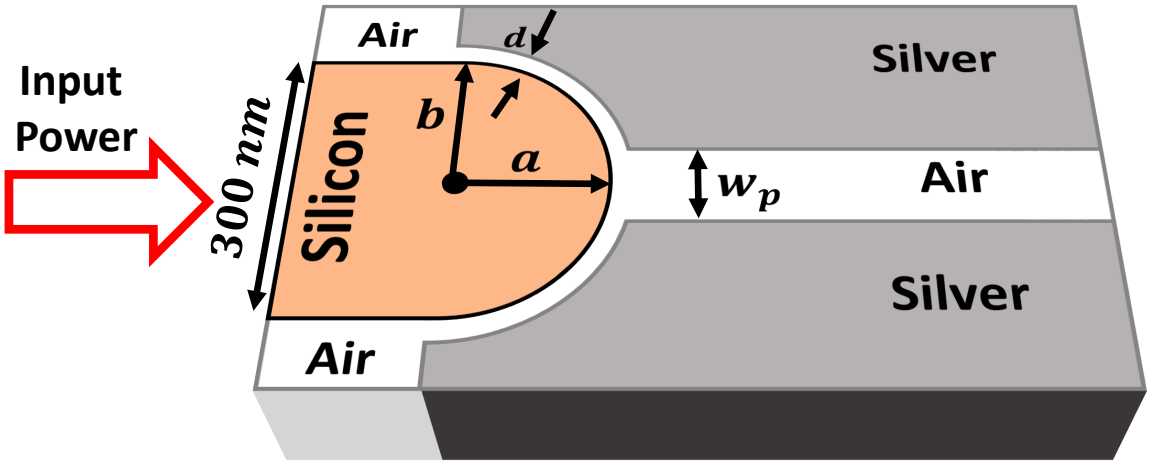

Figure 3.1: Three dimensional view of the proposed air gap based Semi-Elliptical Nanoplasmonic Coupler

The height of the coupler is taken to be 300 nm making it compatible with the width of the dielectric waveguide. The width of the dielectric waveguide is choosen to be 300nm as per the analysis made by G. Veronis *et al.* [19]. The width of the air gap between the metals of the plasmonic waveguide is represented by w_p, whereas the width of the air gap between the two waveguides is represented by d, as shown in fig. 3.1. The semi-elliptical coupling structure has a semi-minor axis and a semi-major axis, lengths of which are defined by the parameters a and b. The relationship between these two parameters can be obtained from the general expression of an ellipse, denoted by the following equation.

$$\frac{x^2}{a^2} + \frac{y^2}{b^2} = 1 \tag{3.1}$$

Where, semi-minor axis length, a, is less then semi-major axis length, b. Length of b is kept fixed at 300 nm for all different simulations. Our main point of interest among all different parameters are the semi-minor axis length (a), width of the air gap between the two waveguides (d) and width of the air gap between the metals of the plasmonic waveguide (w_p). By observing the variation of coupling efficiency with all of these parameters, the optimal dimensions of the coupling structure is obtained. Silicon is used in the coupling structure to couple light into the MDM sub-wavelength plasmonic waveguide from the dielectric waveguide.

3.3 Simulations

3.3.1 Simulation Methods

For investigating the properties of the proposed coupler, Finite Integration Technique (FIT) [24] has been used. FIT is a spatially discretized scheme for solving electromagnetic field problems numerically in both frequency and time domain. Vi-

tal topological properties of different continuous equations like conservation of energy and charge are preserved in FIT, which is important for our case. FIT is the basis for different simulation tools as it covers almost full range of optical applications and electromagnetics. Three-dimensional electromagnetic (EM) simulation software, CST MICROWAVE STUDIO® (CST MWS) is used as the simulation tool. Time domain solver has been used in our simulation. CST MWS in time domain provides the scope of using experimental data directly in the case of frequency dependent dielectric constant of metals (such as silver, gold etc.) [25].

All the boundaries of the proposed structure in the simulation domain are kept open to get the advantages of perfectly matched layer (PML) [26] as well as to prevent back reflections after attenuating fields within the boundary regions. Fundamental mode has been excited at the input terminal to investigate different performance parameters like coupling efficiency, transmission and reflection coefficients, absorbance, VSWR, and return loss. Using different ports, power has been measured at the waveguides acting as the input and output. The received power is measured from just after the interface of the MDM and plasmonic waveguide. As a precaution to avoid the contributions of radiative modes in the measured power, a small distance has been considered while placing the ports besides the interface.

3.3.2 Experimental Validation

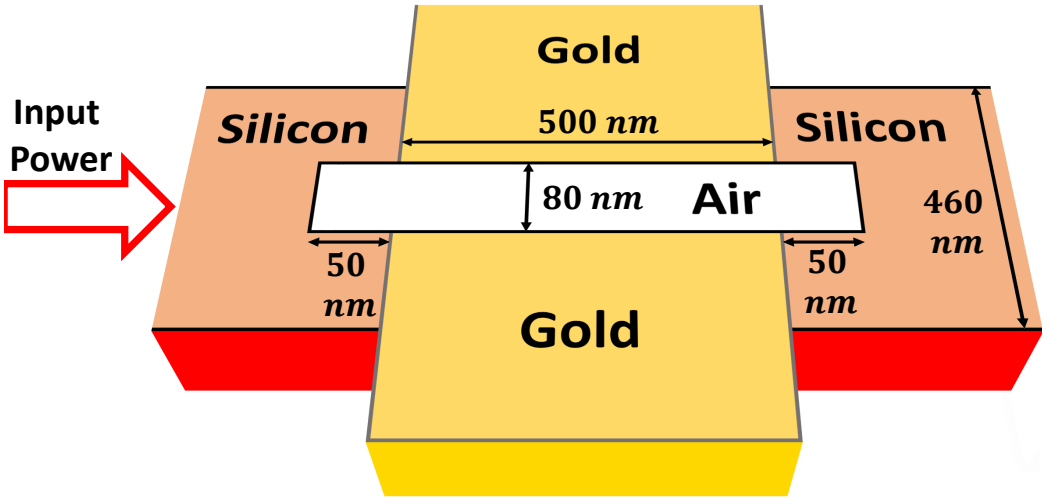

(a)

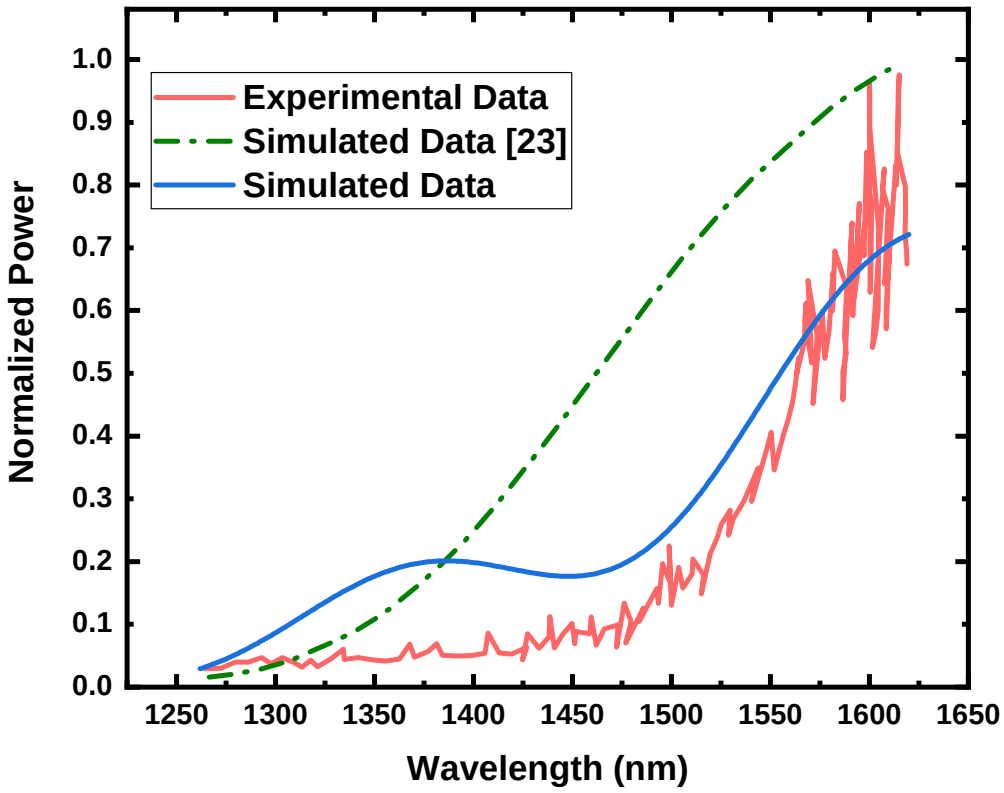

(b)

Figure 3.2: (a) Three dimensional view of Plasmonic Air-Slot Coupler [23] and (b) Comparison of the experimental [23] and simulation results (without 110nm shift) of the Plasmonic Air-Slot Coupler

To validate our simulation, the air-slot coupler proposed by Rami A. Wahsheh *et al.* [23] has been re-simulated. The two-dimensional finite-difference-time-domain (FDTD) method has been used in their design and analysis. Due to the long run time and large memory requirements for 3D simulations, Rami A. Wahsheh *et al.* [23] performed 2D FDTD simulation and compared their result with the results obtained through the analysis of a 3D experimental structure. Using FIT, we have successfully simulated the experimental structure of Rami A. Wahsheh, which shows excellent agreement with experimental data, particularly within the wavelength range (1500 to 1620 nm). The dielectric material and metal that they have used are silicon and gold respectively. The geometry of the experimental structure that has been simulated is shown in fig. 3.2(a).

The coupling efficiency has been analyzed by normalizing the output power with respect to the input power. Variation of normalized power with wavelength has been demonstrated in fig. 3.2(b). Experimental spectrum of the fabricated plasmonic coupler is analogous to that of simulation of Rami A. Wahsheh *et al.* [23] when shifted to 110 nm due to lithography and etching bias. Here, we did not consider the 110 nm shift in our simulation. The percentage of error at different wavelengths has been tabulated in Table 3.1.

Table 3.1: Percentage of error of simulated data and experimental data between wavelengths 1500 nm to 1620 nm

Wavelength	**Experimental Data [23]**	**Simulated Data**	**Error (%)**
1500	0.224	0.255	13.839
1528	0.288	0.340	18.056
1545	0.381	0.448	17.585
1550	0.406	0.476	17.241
1567	0.545	0.557	2.202
1576	0.598	0.599	0.167
1581	0.620	0.623	0.484
1592	0.638	0.657	2.978
1597	0.687	0.672	2.183
1610	0.708	0.711	0.424
1618	0.718	0.719	0.139
1620	0.720	0.721	0.139
Average Error			**6.286**

3.4 Results and Discussion

3.4.1 Obtaining Optimal Dimensions

With the view to obtaining the optimal Semi-minor axis length (a) of the semi-elliptical structure, we varied a from 0 nm (vertical line) to 150 nm (semi-circle) with 10 nm step size, to get the plot of all different coupling efficiencies against wavelength within the wavelength range of 800 nm to 2200 nm. These are depicted in fig. 3.3(a). Coupling efficiency at 1.55 μm has been plotted against a in fig. 3.3(b).

Analyzing fig. 3.3(b), we observe that at a semi-minor axis length, $a = 100$ nm the coupling efficiency is maximum ($\sim$ 83%) at the optical communication wavelength (1.55 μm). After that, optimized air gap between the two waveguides (i.e. d) has been determined by varying d from 0 nm (neglecting air gap) to 50 nm with 5 nm step size and observing the corresponding coupling efficiency. The optimum value of d is obtained from coupling efficiency vs air gap between the two waveguides as observed in fig. 3.4(a).

From fig. 3.4(a), it is seen that only air gap of width 5 nm in between the two waveguides provide maximum coupling efficiency of $\sim$ 83%. Thus the optimum value of d is 5 nm. To get the optimum width of the air gap between the metals of the plasmonic waveguide (i.e. w_p), w_p was varied from 0 nm to 150 nm with 10 nm step size and the corresponding coupling efficiency has been recorded. From the plot of coupling efficiency vs width of the air gap between the metals of the plasmonic waveguide (i.e. w_p) depicted in fig. 3.4(b), we get 50 nm as the optimum value of w_p.

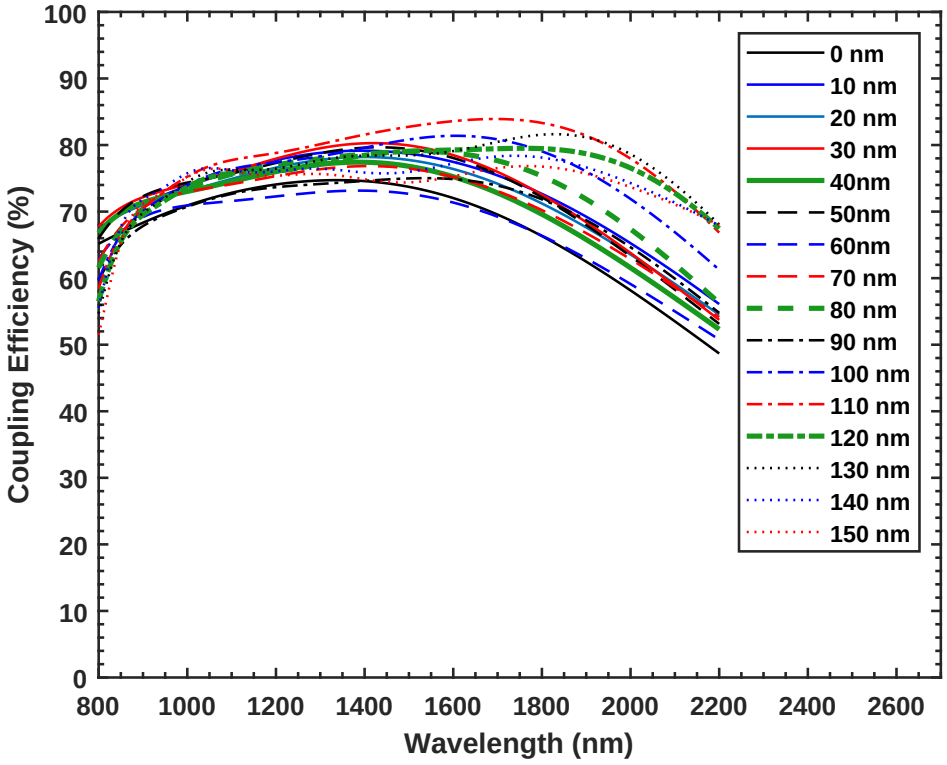

(a)

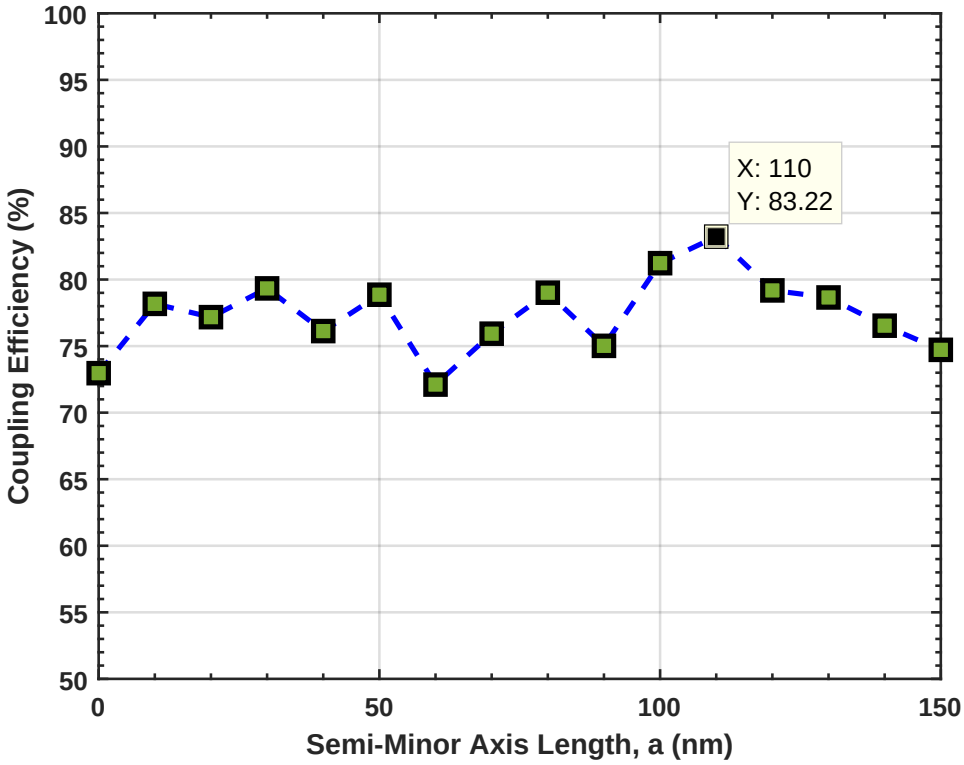

(b)

Figure 3.3: (a) Coupling efficiency vs wavelength and (b) Coupling efficiency vs semi-minor axis length to find optimal value of a at optical communication wavelength (1.55 μm))

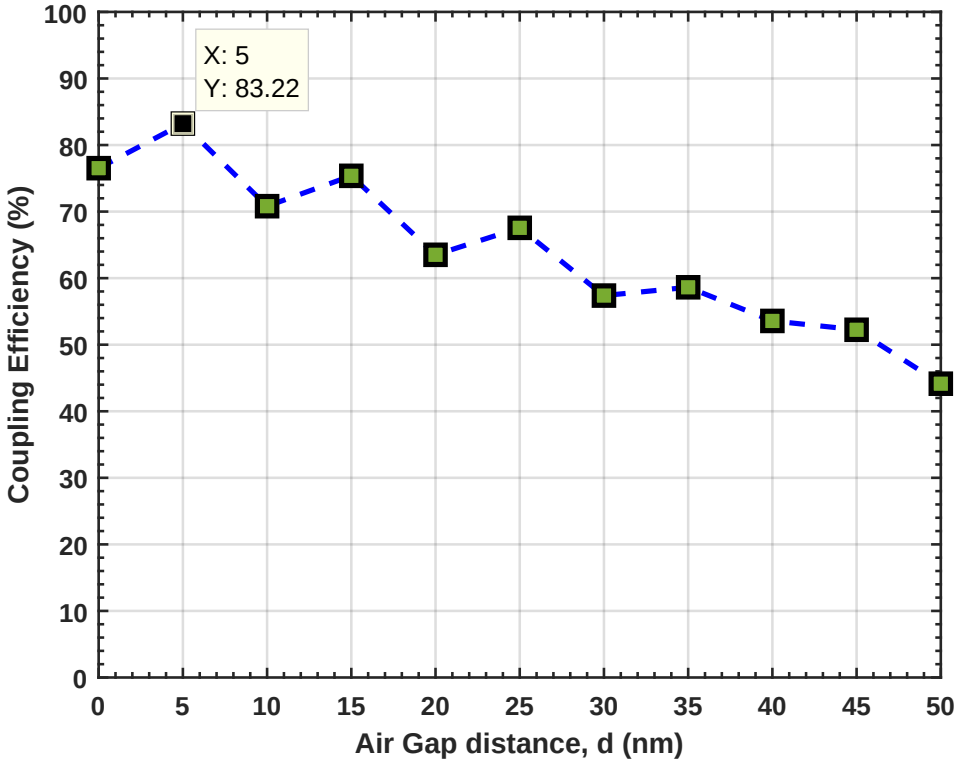

(a)

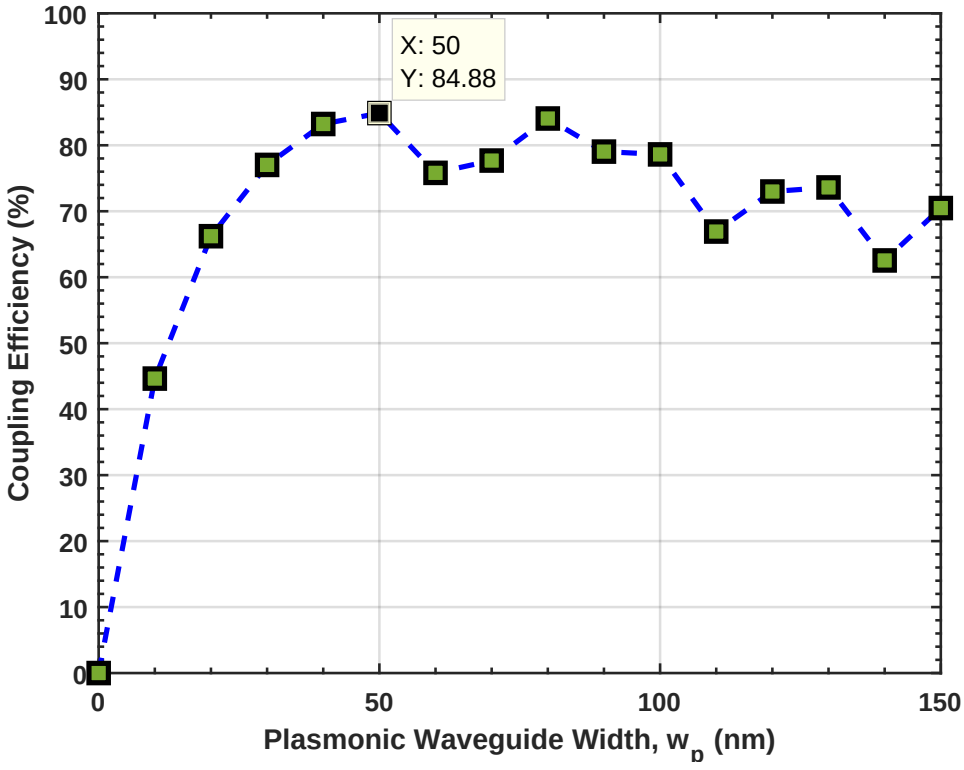

(b)

Figure 3.4: (a) Coupling efficiency vs air gap between the two waveguides, d and (b) Coupling efficiency vs width of the air gap between the metals of plasmonic waveguide, w_p at optical communication wavelength (1.55 μm)

Table 3.2: Summary of dimensions of the optimized nanoplasmonic coupler

Dimension	**Value**
Semi-minor axis length, a	110 nm
Air gap width, d	5 nm
Width of the plasmonic waveguide, w_p	50 nm

3.4.2 Performance of the Optimized Coupler

Using the optimal dimensions demonstrated in table 3.2, the proposed nanoplasmonic semi-elliptical coupler has been simulated to obtain different performance parameters such as normalized power, coupling efficiency, reflection coefficient, return loss, and VSWR for a wavelength range of 800 nm to 2000 nm.

Fig. 3.5(a) shows the Electric field distribution at the communication wavelength (1.55 μm). Colorimetric change with respect to the electric field and x, y, and z directions are shown on the inset. It also gives visual perception of how efficient the proposed coupler is in terms of coupling. Fig. 3.5(b) shows the variation of normalized transmitted power, reflected power and absorbed power with the wavelength. At 1.55 μm, we have found normalized reflectance ($\sim$ 0.056) and absorbance ($\sim$ 0.095) to be very small. On the other hand, the obtained normalized transmittance ($\sim$ 0.849) is found to be much large. Also, it is observed that the sum of these three quantities is $\sim$ 1.

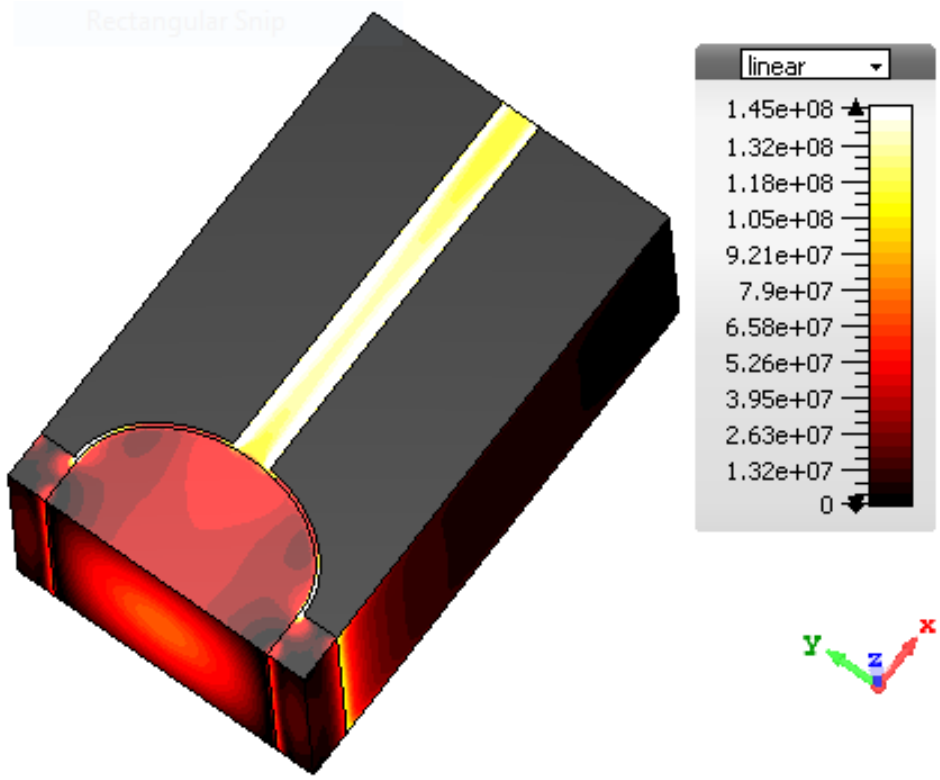

(a)

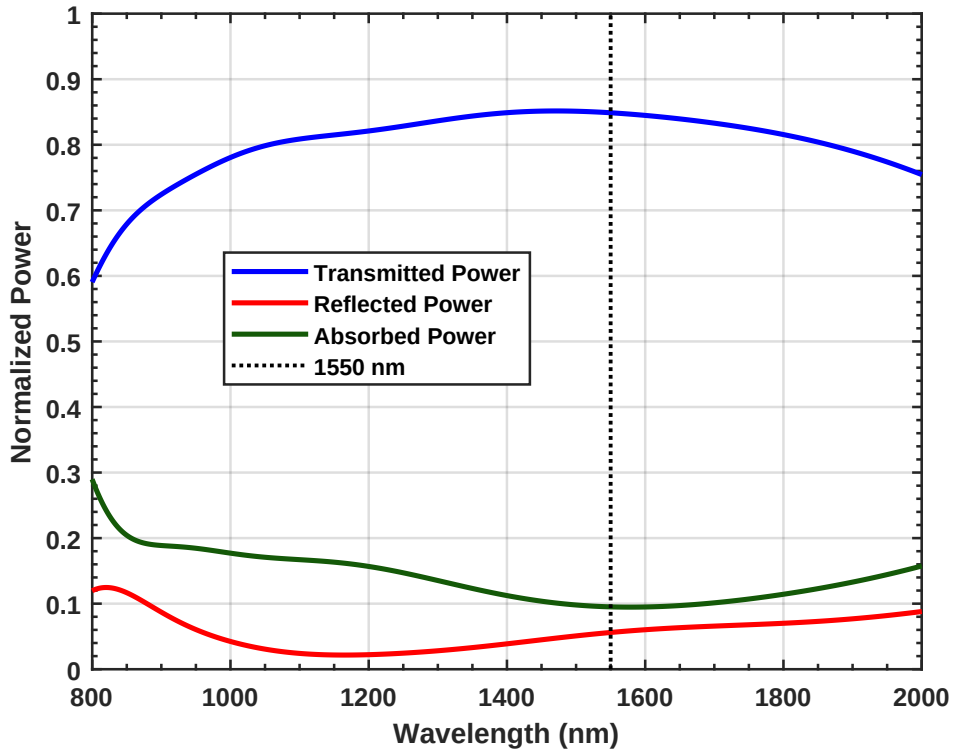

(b)

Figure 3.5: (a) Electric field profile (E_y) of the proposed air gap based semi-elliptical nanoplasmonic coupler at optical communication wavelength (1.55 μm) and (b) Normalized transmitted power, reflected power, and absorbed power vs wavelength of optimized proposed coupler

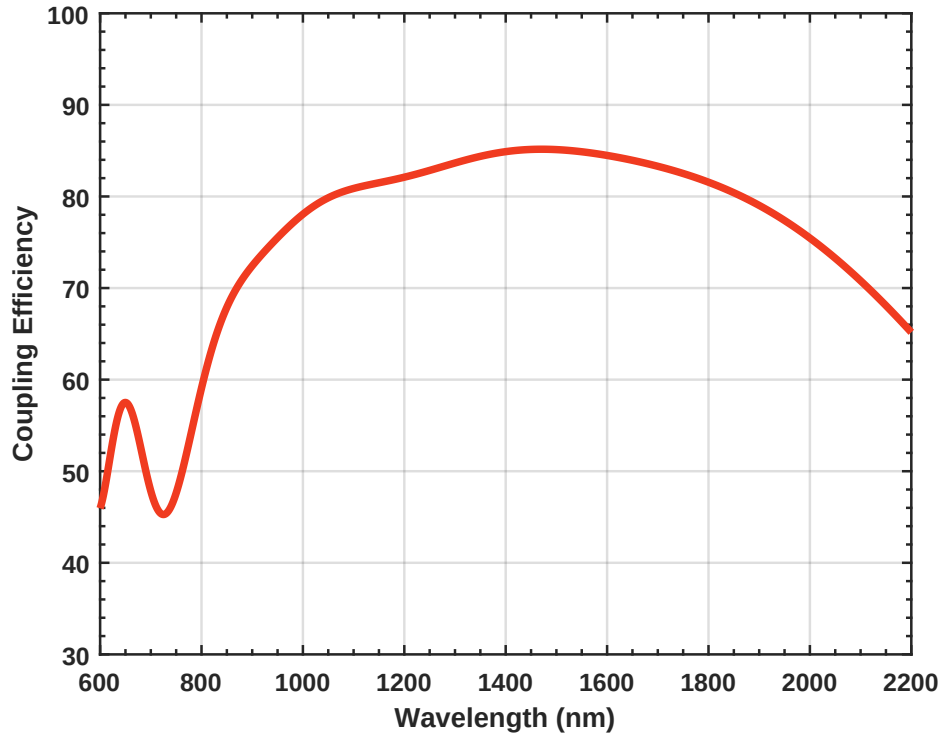

(a)

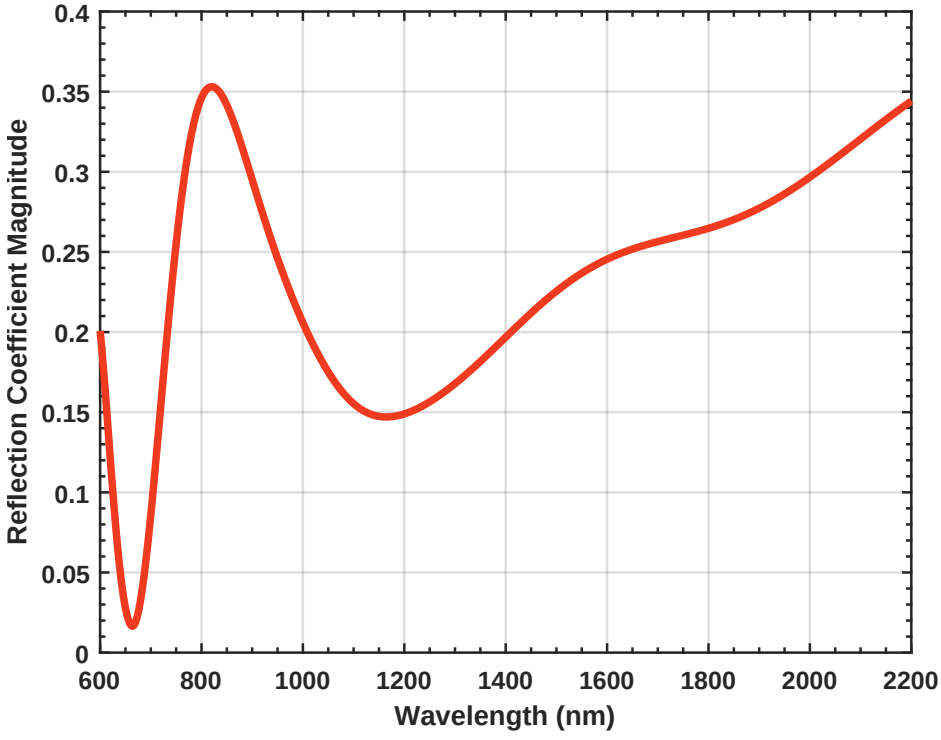

(b)

Figure 3.6: (a) Coupling efficiency vs wavelength analysis of the optimized coupler and (b) Reflection coefficient vs wavelength of optimized proposed coupler

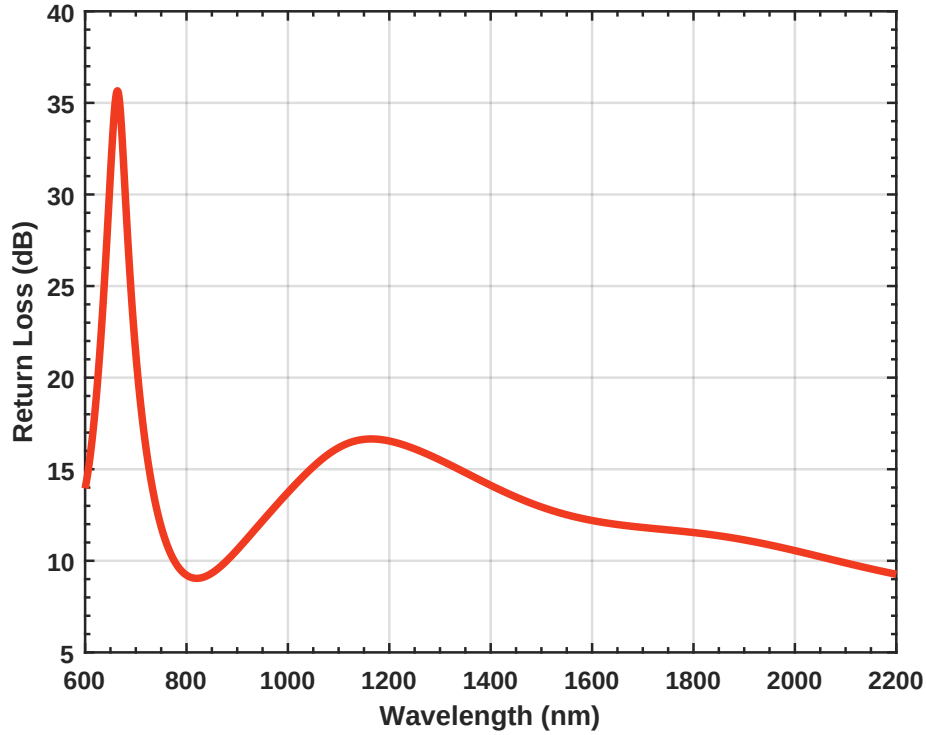

(a) •

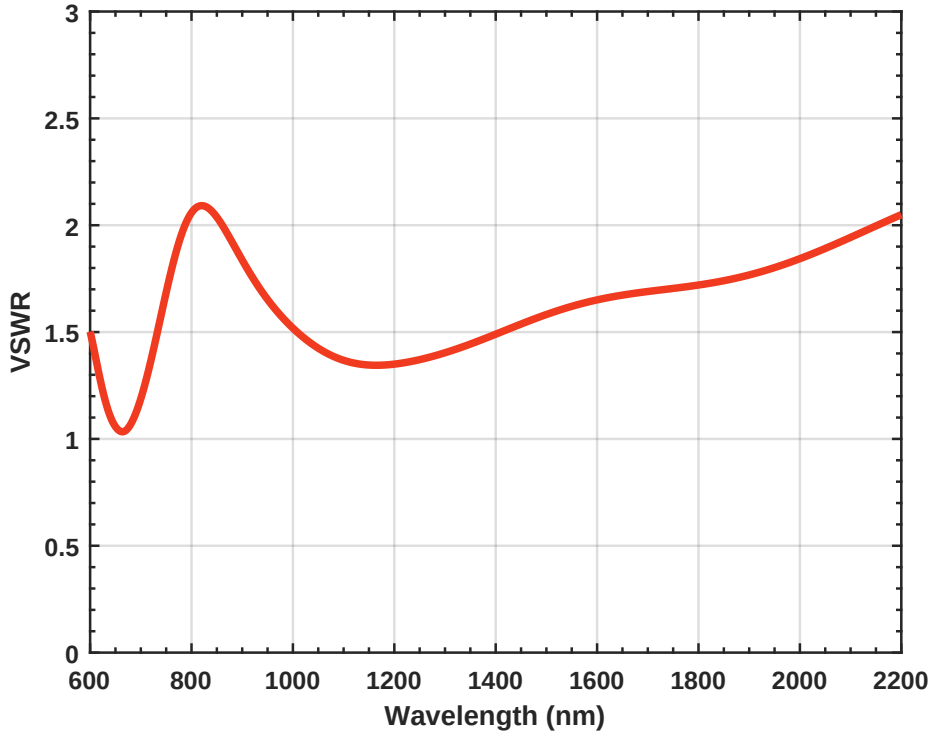

(b) •

Figure 3.7: (a) Return loss vs wavelength of the optimized coupler and (b) VSWR (Voltage Standing Wave Ratio) vs wavelength of optimized proposed coupler

Fig. 3.6(a) shows the coupling efficiency variation with the change of wavelength from 600 nm to 2200 nm. The coupling efficiency at the optical communication wavelength (1.55 μm) for the proposed coupler has been found to be $\sim$ 85%. It is also observed that the coupling efficiency is considerably large for a broad range of wavelengths. It is above 80% from 1010 nm to 1810 nm. Fig. 3.6(b) shows the reflection coefficient variation with the change of wavelength. A reflection coefficient of $\sim$ 0.23 is found at 1.55 μm.

Fig. 3.7(a) shows the return loss variation with the change of wavelength. At 1.55 μm the value of the return loss is found to be 12.51 dB which is more than the minimum acceptable value of the return loss (tyically 10 dB). The obtained return loss indicates lower impedance mismatch at the optical communication wavelength. Fig. 3.7(b) shows the VSWR variation with the change of wavelength. At 1.55 μm, the value of the VSWR is found to be $\sim$ 1.621 which is acceptable as it is less than 2.00. Since, smaller the value of VSWR, the more power is delivered (minimum value of VSWR is 1.0).

Table 3.3: Summary of different performance parameters of the optimized nanoplasmonic coupler at 1.55 μm

Performance Parameter	**Value**
Transmittance	0.8488
Reflectance	0.0561
Absorbance	0.0951
Reflection Coefficient Magnitude	0.237
Return Loss	12.51 dB
VSWR	1.624

3.4.3 Tolerance to Angular and Air Gap Misalignment

Tolerance to angular and air gap misalignment are two very attractive features of our proposed coupler which can give flexibility to the fabrication process. It has been observed by varying the angular alignment from 0° to ±5° and it is found to give coupling efficiency above 77% and the values are summarized in table 3.4. Fig. 3.8 shows the schematic when angular misalignment is considered, α represents the angle to which the misalignment has been considered.

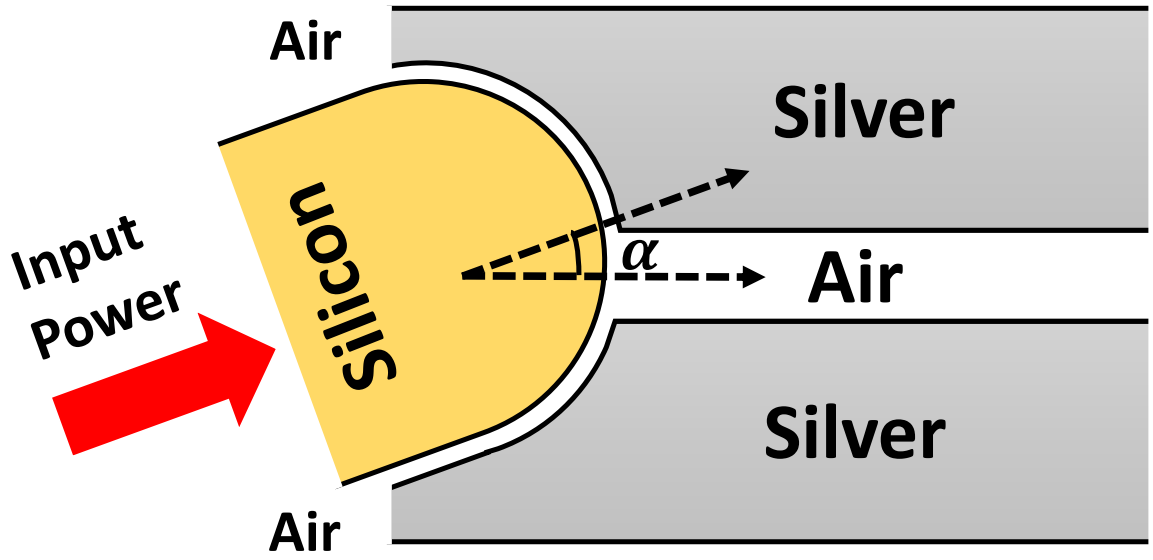

Figure 3.8: Angular misalignment (top view) between the axis of two couplers defined by the parameter α

Angular Alignment	Value
0° (no misalignment)	84.88%
+5°	78.20%
−5°	77.00%

Table 3.4: Tolerance limit of angular misalignment and value of coupling efficiency at 1.55 μm

Tolerance to air gap misalignment between the two waveguides (d) is depicted in fig. 3.9. We have considered the situation when the air gap between the two waveguides, d, is not uniform (i.e. $d_1 \neq d_2$). Three cases are analyzed; when there is no misalignment (i.e. $d_1 = d_2$), when there is a horizontal shift in d_1 by 10 nm (i.e. $d_1 > d_2$), and when there is a vertical shift in d_2 by 10 nm (i.e. $d_1 < d_2$). The corresponding tolerance limit is demonstrated in table 3.5.

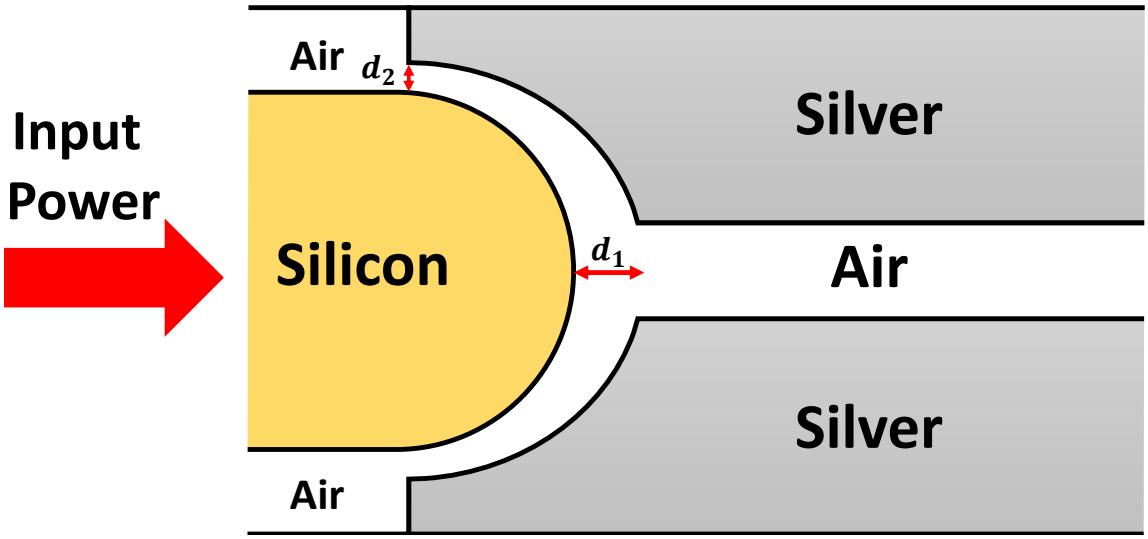

Figure 3.9: Top view of the air gap misalignment between the axis of two couplers defined by d_1 and d_2

Air Gap Alignment	Value
$d_1 = d_2$	84.88%
$d_1 > d_2$	76.50%
$d_1 < d_2$	71.20%

Table 3.5: Tolerance limit of air gap misalignment and value of coupling efficiency at 1.55 μm

3.4.4 Comparison of result

Table 3.6: Coupling effiency of different couplers

Coupler Type	**Coupling Efficiency**
Si based rectangular coupler [19]	56%
CuO based rectangular coupler [27]	56%
AlAs based rectangular coupler [28]	60%
Alumina (Al_2O_3) based rectangular coupler [28]	50%
GLS based rectangular coupler [29]	67%
Si based Semi-Elliptical Coupler with Air Gap	85%

Chapter 4

Conclusion

As a promising sub-discipline of nano-photonics, plasmonics has attracted much attention in recent years. Photonic devices with considerably smaller dimensions compared to the wavelength of propagating light is the magnificent outcome of plasmonics. One of the subsequent requirement is an efficient coupler between dielectric and MDM waveguide. With the view to fulfilling this requirement, in this paper we propose a novel design of nanoplasmonic coupling structure along with the analysis of different performance parameters like coupling efficiency, reflection coefficient, VSWR and return loss. Optimum dimensions of the coupler are achieved after variation of the air gap of Ag-Air-Ag waveguide, curvature of semi-elliptical structure, width of air gap in between two waveguides. Optimized Coupler which is proposed provides a coupling efficiency of $\sim 85\%$. Distinctive features of the proposed coupler are broad range of operating frequency, tolerance to angular and air gap misalignment giving flexibility to fabrication process. It is expected that the proposed structure along with the analysis will open up new dimensions in the efficient plasmonic coupler design.

References

[1] E. Ozbay, Plasmonics: Merging photonics and electronics at nanoscale dimensions, Science 311 (5758) (2006) 189–193. doi:10.1126/science.1114849.
URL https://doi.org/10.1126%2Fscience.1114849

[2] R. F. Oulton, V. J. Sorger, D. A. Genov, D. F. P. Pile, X. Zhang, A hybrid plasmonic waveguide for subwavelength confinement and long-range propagation, Nature Photonics 2 (8) (2008) 496–500. doi:10.1038/nphoton.2008.131.
URL https://doi.org/10.1038%2Fnphoton.2008.131

[3] D. K. Gramotnev, S. I. Bozhevolnyi, Plasmonics beyond the diffraction limit, Nature Photonics 4 (2) (2010) 83–91. doi:10.1038/nphoton.2009.282.
URL https://doi.org/10.1038%2Fnphoton.2009.282

[4] S. Kawata, Y. Inouye, P. Verma, Plasmonics for near-field nano-imaging and superlensing, Nature Photonics 3 (7) (2009) 388–394. doi:10.1038/nphoton.2009.111.
URL https://doi.org/10.1038%2Fnphoton.2009.111

[5] K. A. Willets, R. P. V. Duyne, Localized surface plasmon resonance spectroscopy and sensing, Annual Review of Physical Chemistry 58 (1) (2007) 267–297. doi:10.1146/annurev.physchem.58.032806.104607.
URL https://doi.org/10.1146%2Fannurev.physchem.58.032806.104607

[6] K. R. Catchpole, A. Polman, Plasmonic solar cells, Optics Express 16 (26) (2008) 21793. doi:10.1364/oe.16.021793.
URL https://doi.org/10.1364%2Foe.16.021793

[7] J. Henzie, M. H. Lee, T. W. Odom, Multiscale patterning of plasmonic metamaterials, Nature Nanotechnology 2 (9) (2007) 549–554. doi:10.1038/nnano.2007.252.
URL https://doi.org/10.1038%2Fnnano.2007.252

[8] S. J. Tan, M. J. Campolongo, D. Luo, W. Cheng, Building plasmonic nanostructures with DNA, Nature Nanotechnology 6 (5) (2011) 268–276. doi:10.1038/nnano.2011.49.
URL https://doi.org/10.1038%2Fnnano.2011.49

[9] S. Yang, X. Ni, X. Yin, B. Kante, P. Zhang, J. Zhu, Y. Wang, X. Zhang, Feedback-driven self-assembly of symmetry-breaking optical metamaterials in solution, Nature Nanotechnology 9 (12) (2014) 1002–1006. doi:10.1038/nnano.2014.243.
URL https://doi.org/10.1038%2Fnnano.2014.243

[10] S. A. Maier, P. E. Barclay, T. J. Johnson, M. D. Friedman, O. Painter, Low-loss fiber accessible plasmon waveguide for planar energy guiding and sensing, Applied Physics Letters 84 (20) (2004) 3990–3992. doi:10.1063/1.1753060.
URL https://doi.org/10.1063%2F1.1753060

[11] L. Chen, J. Shakya, M. Lipson, Subwavelength confinement in an integrated metal slot waveguide on silicon, Optics Letters 31 (14) (2006) 2133. doi:10.1364/ol.31.002133.
URL https://doi.org/10.1364%2Fol.31.002133

[12] R. F. Oulton, G. Bartal, D. F. P. Pile, X. Zhang, Confinement and propagation characteristics of subwavelength plasmonic modes, New Journal of Physics 10 (10) (2008) 105018. doi:10.1088/1367-2630/10/10/105018.
URL https://doi.org/10.1088%2F1367-2630%2F10%2F10%2F105018

[13] B. Steinberger, A. Hohenau, H. Ditlbacher, A. L. Stepanov, A. Drezet, F. R. Aussenegg, A. Leitner, J. R. Krenn, Dielectric stripes on gold as surface plasmon waveguides, Applied Physics Letters 88 (9) (2006) 094104. doi:10.1063/1.2180448.
URL https://doi.org/10.1063%2F1.2180448

[14] N. Fang, Sub-diffraction-limited optical imaging with a silver superlens, Science 308 (5721) (2005) 534–537. doi:10.1126/science.1108759.
URL https://doi.org/10.1126%2Fscience.1108759

[15] J. Rho, Z. Ye, Y. Xiong, X. Yin, Z. Liu, H. Choi, G. Bartal, X. Zhang, Spherical hyperlens for two-dimensional sub-diffractional imaging at visible frequencies, Nature Communications 1 (9) (2010) 143. doi:10.1038/ncomms1148.
URL https://doi.org/10.1038%2Fncomms1148

[16] M. G. Saber, R. H. Sagor, A. A. Noor, M. T. Al-Amin, Numerical investigation of SPP propagation at the nano-scale MDM waveguides with a combiner, Photonics Letters of Poland 5 (3). doi:10.4302/plp.2013.3.12.
URL https://doi.org/10.4302%2Fplp.2013.3.12

[17] R. A. Wahsheh, Z. Lu, M. A. G. Abushagur, Nanoplasmonic couplers and splitters, Optics Express 17 (21) (2009) 19033. doi:10.1364/oe.17.019033.
URL https://doi.org/10.1364%2Foe.17.019033

[18] J.-C. Weeber, Y. Lacroute, A. Dereux, E. Devaux, T. Ebbesen, C. Girard, M. U. González, A.-L. Baudrion, Near-field characterization of bragg mirrors engraved in surface plasmon waveguides, Physical Review B 70 (23). doi:10.1103/physrevb.70.235406.
URL https://doi.org/10.1103%2Fphysrevb.70.235406

[19] G. Veronis, S. Fan, Theoretical investigation of compact couplers between dielectric slab waveguides and two-dimensional metal-dielectric-metal plasmonic waveguides, Optics Express 15 (3) (2007) 1211. doi:10.1364/oe.15.001211.
URL https://doi.org/10.1364%2Foe.15.001211

[20] R. A. Wahsheh, Z. Lu, M. A. G. Abushagur, Nanoplasmonic air-slot coupler: Design and fabrication, in: Frontiers in Optics 2012/Laser Science XXVIII, OSA, 2012. doi:10.1364/fio.2012.fth4a.6.
URL https://doi.org/10.1364%2Ffio.2012.fth4a.6

[21] P. Ginzburg, M. Orenstein, Plasmonic transmission lines: from micro to nano scale with $\lambda/4$ impedance matching, Optics Express 15 (11) (2007) 6762. doi:

10.1364/oe.15.006762.
URL https://doi.org/10.1364%2Foe.15.006762

[22] D. F. P. Pile, D. K. Gramotnev, Adiabatic and nonadiabatic nanofocusing of plasmons by tapered gap plasmon waveguides, Applied Physics Letters 89 (4) (2006) 041111. doi:10.1063/1.2236219.
URL https://doi.org/10.1063%2F1.2236219

[23] R. A. Wahsheh, M. A. G. Abushagur, Experimental and theoretical investigations of an air-slot coupler between dielectric and plasmonic waveguides, Optics Express 24 (8) (2016) 8237. doi:10.1364/oe.24.008237.
URL https://doi.org/10.1364%2Foe.24.008237

[24] T. Weiland, A discretization method for the solution of maxwell's equations for six-component fields.-electronics and communication,(aeü), vol. 31.

[25] E. D. Palik, Handbook of Optical Constants of Solids, Author and Subject Indices for Volumes I, II, and III, Elsevier, 1998.

[26] J.-P. Berenger, A perfectly matched layer for the absorption of electromagnetic waves, Journal of Computational Physics 114 (2) (1994) 185–200. doi:10.1006/jcph.1994.1159.
URL https://doi.org/10.1006%2Fjcph.1994.1159

[27] M. G. Saber, R. H. Sagor, Analysis of cuprous oxide-based ultra-compact nanoplasmonic coupler, Applied Nanoscience 5 (2) (2014) 217–221. doi:10.1007/s13204-014-0308-3.
URL https://doi.org/10.1007%2Fs13204-014-0308-3

[28] M. G. Saber, R. H. Sagor, Design and study of nano-plasmonic couplers using aluminium arsenide and alumina, IET Optoelectronics 9 (3) (2015) 125–130. doi:10.1049/iet-opt.2014.0027.
URL https://doi.org/10.1049%2Fiet-opt.2014.0027

[29] M. G. Saber, R. H. Sagor, Design and analysis of a gallium lanthanum sulfide based nanoplasmonic coupler yielding 67% efficiency, Optik 125 (18) (2014)

5374–5377. doi:10.1016/j.ijleo.2014.06.034.
URL https://doi.org/10.1016%2Fj.ijleo.2014.06.034